Organic Crystal Engineering with Piperazine-2,5-diones. 1. Crystal Packing of Piperazinediones Derived from Substituted 2-Aminoindan-2-carboxylic Acids

Lawrence J. Williams, B. Jagadish, Scott R. Lyon, Robin A. Kloster,

Michael D. Carducci, and Eugene A. Mash*

Department of Chemistry, The University of Arizona, Tucson, Arizona 85721-0041

Abstract: We have postulated that molecules engineered to participate in three chemically distinct and linearly independent intermolecular interactions will self-assemble in a predictable fashion. Six prototypes for molecules capable of manifesting such interactions were synthesized from 2-amino-indan-2-carboxylic acid, 2-amino-5,6-dimethylindan-2-carboxylic acid, and 2-amino-4,7-dimethoxyindan-2-carboxylic acid. These piperazinediones were characterized in solution by NMR spectroscopy and in the solid state by X-ray crystallography. "Ladder-like" intermolecular amide-to-amide hydrogen bonding interactions were observed in each case, establishing tape structures parallel to one crystallographic axis. Tape morphology varied depending on the arene substitution pattern and was governed by the development of arene and/or van der Waals contact interactions. © 1999 Elsevier Science Ltd. All rights reserved.

Keywords: Amino acids and derivatives, Indanes, Piperazinones, X-Ray crystal structures

INTRODUCTION

Significant insights into the relationship between molecular structure and packing of organic molecules in the solid state have come from a number of theoretical and experimental studies.[1] It has been clearly established that certain packing motifs are predictable given the presence of complementary atoms[2] or functional groups[3] with proper geometry in a molecule. The relative geometry of atoms and functional groups can be controlled by attachment to suitable molecular scaffolds. The piperazine-2,5-dione ring is a particularly appealing scaffold that has recently drawn attention.[1e,4,5] Our initial crystal engineering efforts based on the piperazinedione scaffold derived from 2-amino-indan-2-carboxylic acid derivatives are presented and discussed in this and the accompanying article in this issue.[6]

Our hypothesis is that suitable chiral molecules can be engineered to engage in three linearly independent intermolecular interactions and will afford solids with predictable crystal structures and bulk properties. For example, there is a need to orient donor-acceptor substituted arene rings in a parallel fashion so that the molecular dipoles do not cancel.[7] The family of molecules 1 constructed from 2-aminoindan-2-carboxylic acid derivatives seemed ideally suited to such a purpose since conformational restriction reduces the number of possible packing modes, while structural variability permits the introduction of linearly independent functionality, including donor-acceptor substituted arenes.

---

* Corresponding author email emash@u.arizona.edu

1
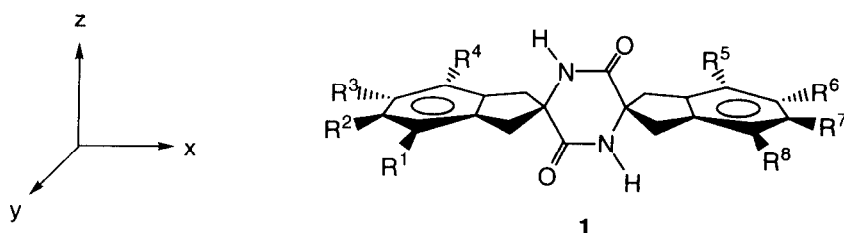
We envisioned that amide–to–amide hydrogen bonding would occur along the z–axis, while intermolecular interactions between the groups R^1, R^4, R^5, and R^8 along the y–axis and between the groups R^2, R^3, R^6, and R^7 along the x–axis could be engineered to achieve predictable order in the crystal. Interactions between the groups R might involve hydrogen bonding, Coulombic, and/or van der Waals contact interactions, depending on the identities of these groups. Piperazinediones **2–7** (Scheme 1) were chosen for initial study as probes of this design model. These compounds were expected to establish the necessary synthetic methodology and to test the reliability of hydrogen bond formation and the effects of arene ring substitution on crystal packing.
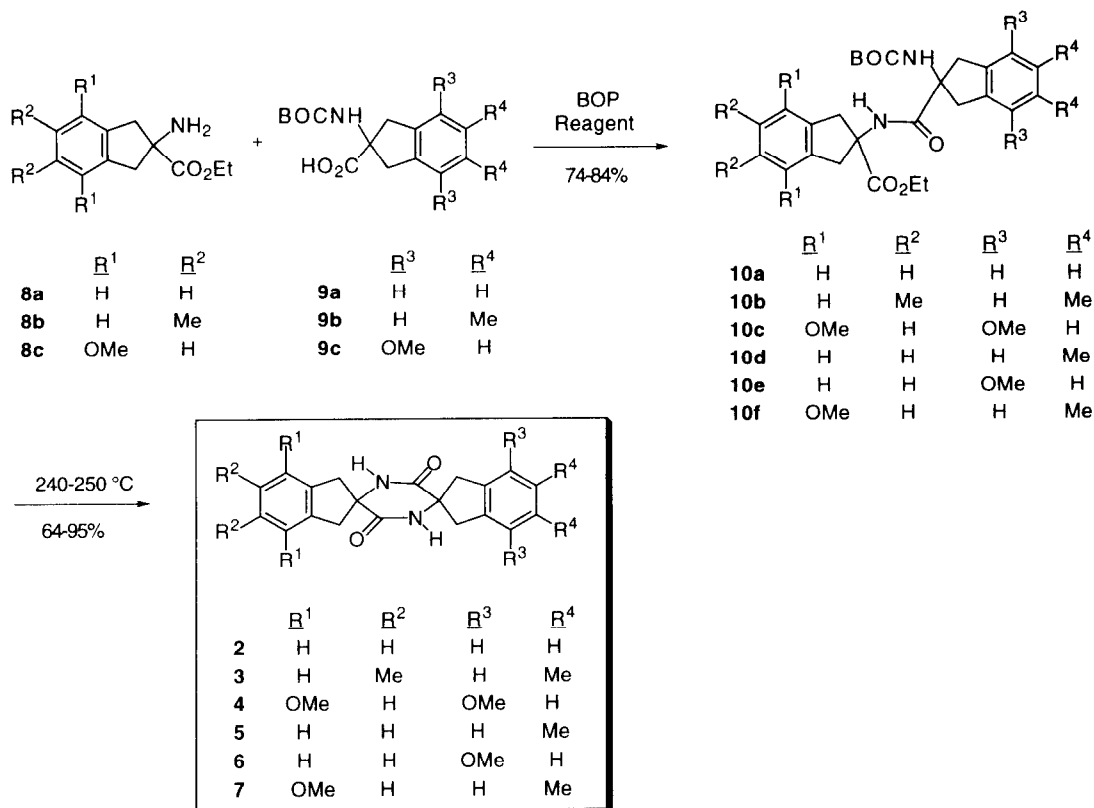
RESULTS

Synthesis and Crystallization

Piperazinediones **2–7** were prepared as depicted in Scheme 1. 2–Aminoindan–2–carboxylic acid derivatives were prepared starting from glycine ethyl ester hydrochloride and substituted α,α'–dibromo–o–xylenes.[8] Coupling of an ethyl 2–aminoindan–2–carboxylate **8** with an N–t–butoxycarbonyl–2–aminoindan–2–carboxylic acid **9** gave the corresponding dipeptide **10**. Thermolysis and recrystallization of the crude products gave the desired piperazinediones. Details of these syntheses are given in the Experimental Section.

Crystals suitable for single crystal x–ray diffraction studies were obtained by recrystallization from hot, dust free solutions of dimethylsulfoxide (DMSO) or mixtures of DMSO and trifluoroacetic acid (TFA). Slow incremental reduction of the solution temperature in a Dewar–oil bath gave the best results, although solutions containing TFA sometimes required cooling below room temperature. Two crystal morphologies, rod–like and pseudo–octahedral, were observed for piperazinedione **4**. Both morphologies were shown to have the same unit cell parameters.

Crystal Structures–Molecular

Crystal structure data is given in Table 1. All compounds crystallized in monoclinic crystal systems. Geometric (conformational) data for piperazinediones **2–7** in the crystals is given in Table 2. Dihedral angles α and β are measures of the degree of non–planarity of the piperazinedione ring (for planar rings $\alpha = \beta = 180°$). The dihedral angle χ is a measure of the degree of non–planarity of the cyclopentene ring component of the indane moiety (for planar rings $\chi = 180°$). The C_4–C_7–O_3–C_{11} torsion angle, δ, measures the orientation of the methoxy substituent relative to the plane of the benzene ring.

	R^1	R^2
8a	H	H
8b	H	Me
8c	OMe	H

	R^3	R^4
9a	H	H
9b	H	Me
9c	OMe	H

	R^1	R^2	R^3	R^4
10a	H	H	H	H
10b	H	Me	H	Me
10c	OMe	H	OMe	H
10d	H	H	H	Me
10e	H	H	OMe	H
10f	OMe	H	H	Me

	R^1	R^2	R^3	R^4
2	H	H	H	H
3	H	Me	H	Me
4	OMe	H	OMe	H
5	H	H	H	Me
6	H	H	OMe	H
7	OMe	H	H	Me

Scheme 1. Synthesis of Piperazinediones 2–7.

NMR spectra of piperazinediones 2–7 measured in TFA–d or DMSO–d_6 were consistent with the expected point group symmetries for these molecules in solution, C_{2h} for 2–4 and C_s for 5–7. However, piperazinedione 2 crystallized in space group $C2/c$. The piperazinedione ring of 2 exists in two enantiomeric pseudo–boat conformations in the crystal. The indane cyclopentene rings of 2 are folded equally and symmetrically toward the respective proximal piperazinedione nitrogen atom. Two–fold rotational molecular symmetry exists, but mirror and inversion molecular symmetries are absent because the piperazinedione ring of 2 is puckered.
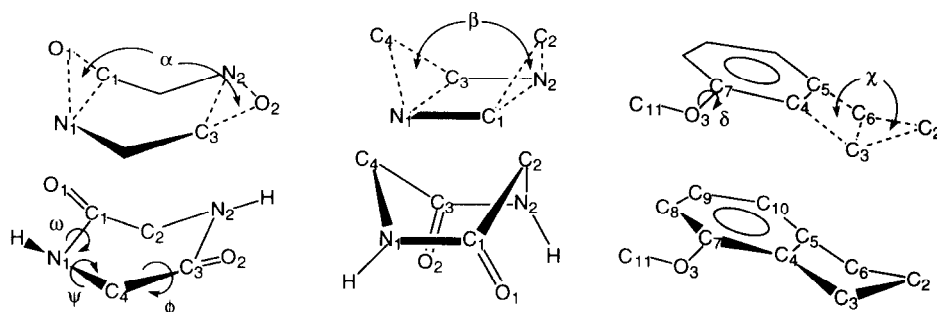
Piperazinedione 3 also crystallized in space group $C2/c$. While the piperazinedione ring of 3 is nearly flat in the crystal ($\alpha_3 = 180°$, $\beta_3 = 180°$), slight symmetrical displacements of C_2 and C_4 to opposite sides of the average plane produce a shallow pseudo–chair conformer. The cyclopentene rings are equally and symmetrically folded toward the proximal nitrogen atoms. Owing to the conformation of the piperazinedione ring and the puckering of the cyclopentene rings, inversion molecular symmetry exists for piperazinedione 3 in the crystal, but rotational and mirror molecular symmetries are absent.

Table 1. Crystallographic Data for Piperazinediones 2–7.

Compound[a]	space group	D/P[b]	Z[c]	a (Å)	b (Å)	c (Å)	β (deg)	R[b]	R_w[b]	density (g/cm³)	V (Å³)	crystal habit	mp (°C)
2	C2/c	13.0	4	9.757(2)	14.014(3)	11.840(1)	95.96(1)	0.042	0.054	1.31	1610.1(5)	rod	322-324
3	C2/c	13.6	4	29.941(2)	6.029(1)	11.620(1)	110.35(6)	0.052	0.084	1.26	1966.7(3)	plate	>400
4	C2	13.5	4	23.940(2)	6.163(1)	15.725(1)	106.98(1)	0.040	0.057	1.31	2218.9(2)	rod	>300 (dec)
5	$P2_1/c$	11.8	8	10.5635(10)	11.0084(10)	31.039(3)	97.922(2)	0.0699	0.1627	1.29	3575.0(6)	plate	316-318
6	$P2_1$	6.6	2	8.4211(1)	6.1538(8)	17.624(2)	96.478(2)	0.0733	0.1502	1.38	907.4(2)	needle	311-312
7	$P2_1/n$	13.0	4	17.3765(18)	6.0596(7)	19.332(2)	101.445(4)	0.0559	0.1365	1.35	1995.1(4)	block	344-346

[a]Structures 2-4 were solved using Molen and structures 5-7 were solved using Shelx. [b]For Molen, R = $|F(\Sigma|F_O - F_C|, \Sigma F_O)$ for $F_O > 3\sigma(F)$ and $R_w = |R(|F|\Sigma w(F_O - F_C)^2, \Sigma wF_O^2))$ where $w = \dfrac{4(F_O^2)}{\sigma^2(F_O^2)}$. For Shelx, $R = \dfrac{\Sigma||F_O|-|F_C||}{\Sigma|F_O|}$ for $F_O > 4\sigma(F)$ and $R_w = \sqrt{\dfrac{\Sigma w(F_O^2 - F_C^2)^2}{\Sigma w(F_O^2)^2}}$ where $w = \dfrac{1}{\sigma^2(F_O^2) + (a \times p)^2 + (b \times p)}$. [b]Data to parameter ratio. [c]Molecules per unit cell.

Table 2. Conformational Data for Piperazinediones **2–7**.[a]

Compound	φ (deg)[b]	ψ (deg)[b]	ω (deg)[b]	α (deg)[c]	β (deg)[c]	χ (deg)[d]	δ (deg)[e]
2[f]	−31.1 31.1	34.8 −34.8	−2.8 2.8	148	125	163	na
3	−11.1 11.1	−12.4 12.4	−13.2 13.2	180	180	150	na
4	6.4 8.0	−12.1 −10.3	2.8 4.7	173	165	145 146	165 −173 172 −165
5a[g,h]	5.2 21.9	−7.2 −26.0	−7.3 12.5	169	155	157 (H) 161 (Me)	na
5b[g,h]	−5.1 −23.1	6.7 26.4	8.5 −12.6	169	155	160 (H) 162 (Me)	
6	16.3 16.6	−25.2 −25.8	8.0 8.5	165	145	143 (H) 145 (OMe)	174 −172
7[i]	−13.6 −18.6	18.2 23.7	−1.5 −7.2	165	149	143 (Me) 144 (OMe)	171 −161

[a]Values are listed for each unique substructural element. [b]The dihedral angles φ, ψ, and ω are the torsion angles defined for conformational analysis of amide bonds in peptides.[9] [c]The dihedral angles α and β were previously defined[5b] and are measures of the degree of non–planarity of the piperazinedione ring (for flat rings α = β = 180°). [d]The dihedral χ is formed by the intersection of the plane defined by C_2, C_3, and C_6 and the the average plane defined by C_3, C_4, C_5, and C_6 and is a measure of the degree of non–planarity of the cyclopentene ring component of the indane moiety (for flat rings χ = 180°). [e]The C_4–C_7–O_3–C_{11} torsion angle, δ, measures the twist of the methoxy substituent relative to the plane of the benzene ring. [f]Tapes consist of alternating conformational enantiomers. [g]Two conformers, **5a** and **5b**, alternate in each hydrogen–bonded tape. [h]Adjacent LNTs and VNTs are enantiomeric; i.e., they are composed of the conformational enantiomers of **5a** and **5b**. [i]The methyl groups of compound **7** are highly disordered in the crystal.

Piperazinedione **4** crystallized in space group $C2$. The piperazinedione ring of **4** exists in a single shallow pseudo–boat conformation in the crystal ($\alpha_4 = 173°$, $\beta_4 = 165°$). The cyclopentene rings are unequally folded toward the respective proximal nitrogen atoms ($\chi_4 = 145°$ and 146°). The torsion angles of the methoxy groups are unique ($\delta_4 = 165°$ and $-173°$ for the methoxy groups on one arene ring and $-165°$ and 172° for the methoxy groups on the other arene ring). Although two–fold rotational symmetry very nearly exists for the pentacyclic core, the combination of the pucker in the piperazinedione ring and the unique methoxy group torsions serve to eliminate all molecular symmetry from **4** in the crystal. Single crystals of **4** are chiral.

Piperazinedione **5** crystallized in space group $P2_1/c$. Enantiomeric pairs of two conformational isomers, **5a** and **5b**, are found in the crystal. The piperazinedione rings of **5a** and **5b** exist in slightly different unsymmetrical pseudo–boat conformations that nearly approximate pseudo–half chairs. Pucker in the piperazinedione rings eliminates molecular mirror symmetry from **5** in the crystal. The cyclopentene rings are folded toward the respective proximal piperazinedione nitrogen atoms, but each to a different extent ($\chi_{5a} = 157°$ and 161° for the unsubstituted and dimethyl substituted indanes, respectively, while $\chi_{5b} = 160°$ and 162°).
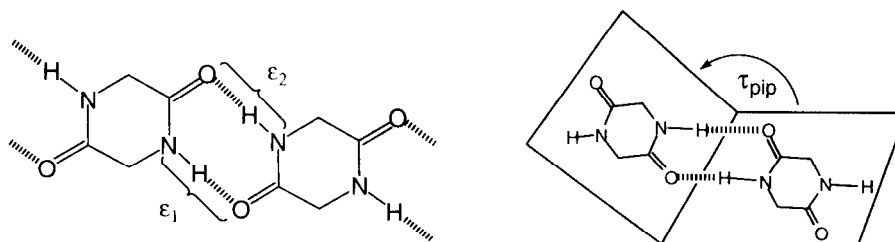
Piperazinedione **6** crystallized in space group $P2_1$. The piperazinedione ring of **6** exists in a single pseudo–twist boat conformation which eliminates molecular mirror symmetry from **6** in the crystal. The cyclopentene rings are unequally folded toward the respective proximal nitrogen atoms and the torsion angles of the methoxy groups are unique ($\delta_6 = 174°$ and $-172°$). Single crystals of **6** are chiral.

Piperazinedione **7** crystallized in space group $P2_1/n$. The piperazinedione ring of **7** exists in enantiomeric shallow pseudo–twist boat conformations in the crystal ($\alpha_7 = 165°$, $\beta_7 = 149°$). This eliminates molecular mirror symmetry from **7** in the crystal. The cyclopentene rings are unequally folded toward the respective proximal nitrogen atoms ($\chi_7 = 143°$ and 144° for the dimethyl and dimethoxy substituted indanes, respectively). The torsion angles of the methoxy groups are unique ($\delta_7 = 171°$ and $-161°$).

Crystal Structures–Supramolecular

The hydrogen bonding properties of piperazinediones **2–7** were expected to play a central role in the establishment of order in the crystalline state.[1e,4,5] From a search of the Cambridge Structural Database (CSD), 46 non–ionic piperazinediones were retrieved, 34 of which were found to form "ladder–like" hydrogen–bonded tapes similar to that diagrammed in Table 3.[10] Structural parameters germane to such hydrogen bonding networks include the N–O interatomic distances, ε_1 and ε_2, which are indicative of the length of the N–H⋯O hydrogen bonds, and the dihedral angle from intersection of the average planes of adjacent piperazinedione rings, τ_p. Values of these structural parameters for piperazinediones **2–7** are given in Table 3, along with average values for tape–forming piperazinediones obtained from the CSD. With the exception of compounds **3** and **5**, these data are in close agreement with the CSD averages and with data from recently published studies.[5]

While each of the piperazinediones **2–7** forms parallel hydrogen–bonded tapes, significantly different tape morphologies are observed depending on the arene ring substitution pattern. Two views of molecules derived from the crystal structures of piperazinediones **2–7** are shown in Table 4. The column labeled "Lateral Neighbor Tapes" (LNTs) presents a view of hydrogen–bonded tapes perpendicular to the hydrogen bonding axis. The column labeled "Vertical Neighbor Tapes" (VNTs) presents two or more pairs of "stacked" LNTs viewed down the hydrogen bonding axis.

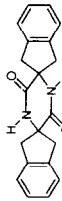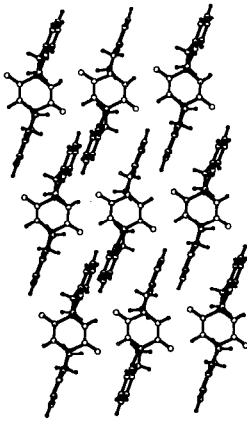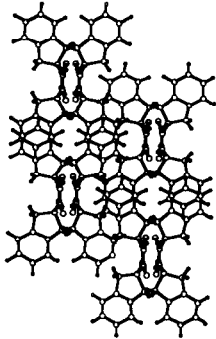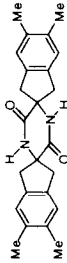**Table 3.** Intermolecular Structural Parameters for Piperazinediones **2–7**: Hydrogen Bonding.[a]
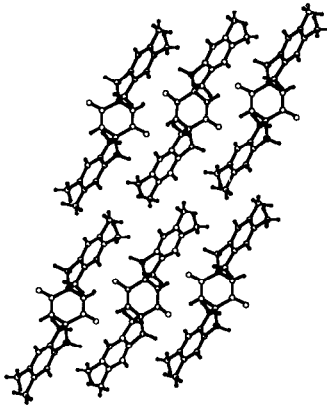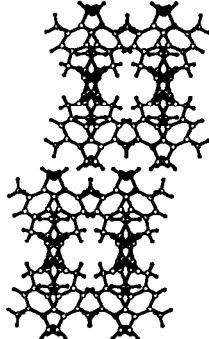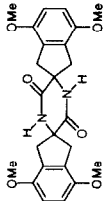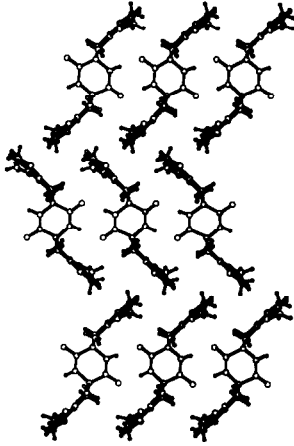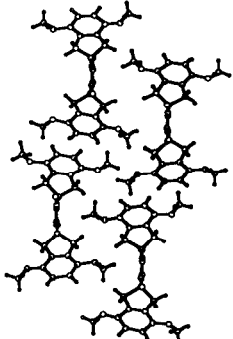
	N–O distances[b]		
Compound	ε_1 (Å)	ε_2 (Å)	τ_p (deg)[c]
2	2.88		0.0
3	2.87		52.4
4	2.85	2.86	0.0
5	2.80	2.94	69.2
	2.82	2.94	
6	2.87	2.87	0.0
7	2.83	2.83	0.0
CSD average	2.89		0.0

[a]Values are listed for each unique substructural element. [b]The distance between the amide nitrogen and oxygen atoms involved in hydrogen bonding. [c]The dihedral τ_p is formed by the intersection of the average planes defined by the atoms of piperazinedione rings adjacent in a tape.

Piperazinedione **2**[6c] was independently prepared and studied by Whitesides and co–workers.[5b] As was described, hydrogen–bonded tapes are composed of alternating conformational enantiomers, producing a "butterfly" motif seen when a tape is viewed down the hydrogen bonding axis (Table 4). As there is little folding of the indane cyclopentene rings, notches exist along the tape edges and directly above the column of piperazinedione rings. LNTs interdigitate to produce arene parallel–displaced face–to–face pairing (seen as arene ring "crossings" in the VNT column of Table 4). Intermolecular geometric parameters, including the arene centroid–to–centroid distance ($\kappa_2 = 3.82$ Å), offset angle ($\zeta_2 = 8.1°$), and tilt angle ($\tau_2 = 12.2°$), are all within the range of values associated with face–to–face interactions (Table 5).[11] Sheets thus formed from LNTs have a dimpled topography with depressions above and below the piperazinedione rings and prominences formed by the interacting arene ring pairs. This topography facilitates van der Waals contact interactions between complementary surfaces in the crystalline solid (see VNT column of Table 4).

For piperazinedione **3**, hydrogen–bonded tapes are composed of a single pseudo–chair conformer of **3** that possesses inversion symmetry. Although the amide hydrogen bond lengths are in keeping with the CSD average, the tape morphology for **3** is unusual in that the average planes of adjacent piperazinedione rings are sharply canted ($\tau_p = 52.4°$). Adjacent molecules within a single hydrogen–bonded tape are related by two–fold rotation. This results in projection of one arene ring of each molecule above the average plane of the hydrogen–

Table 4. Lateral Neighbor Tapes and Vertical Neighbor Tapes for Piperazinediones 2-7.

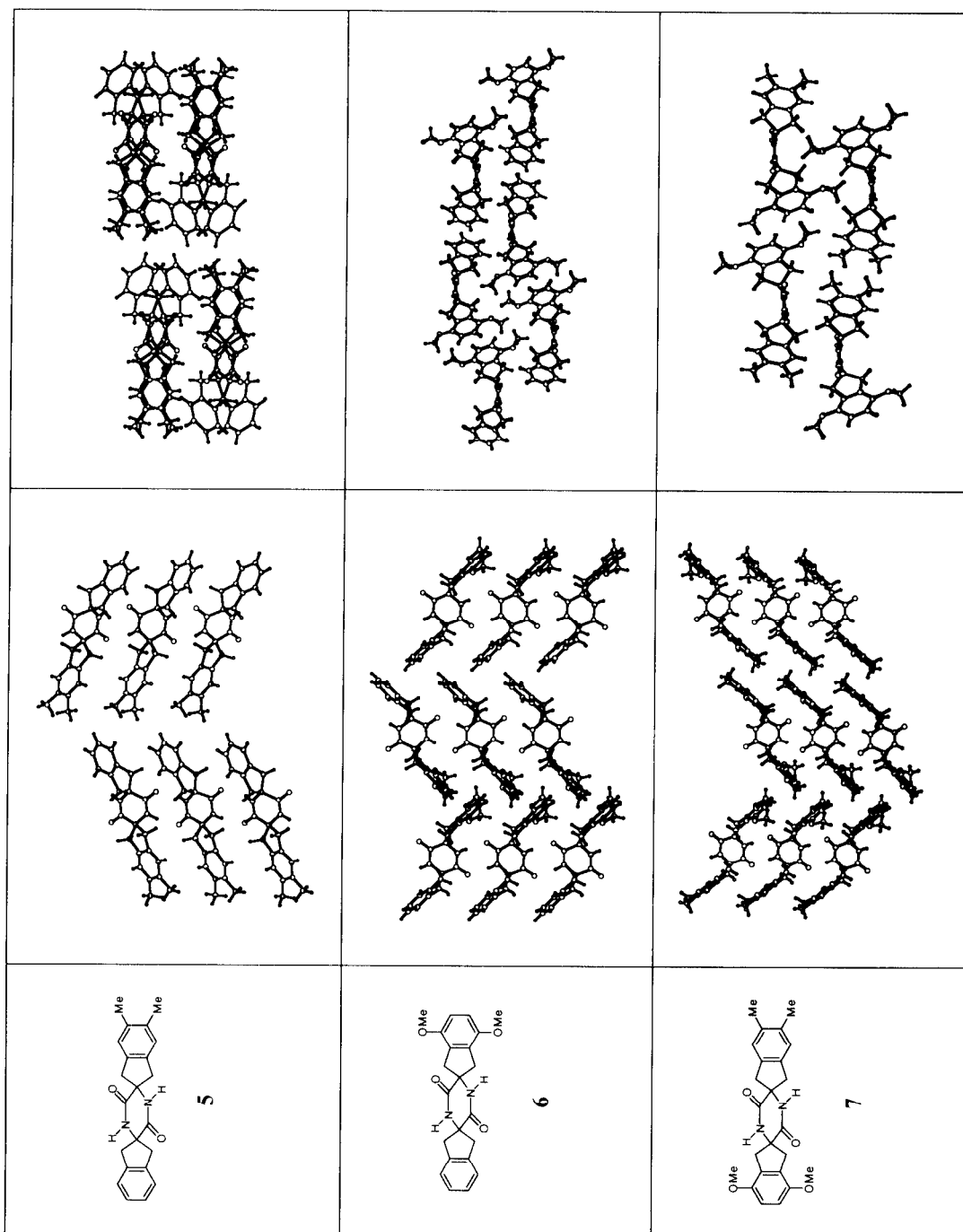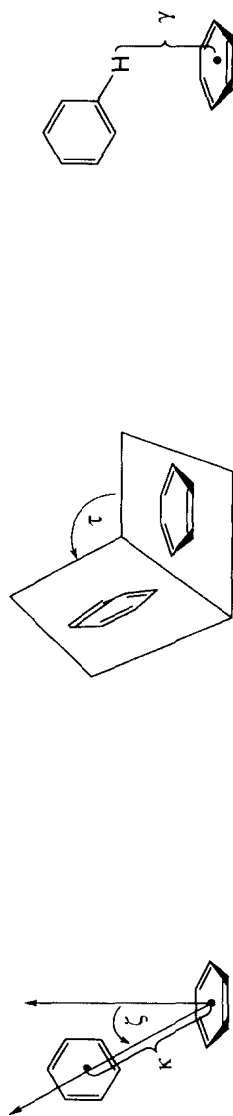| Compound	Lateral Neighbor Tapes	Vertical Neighbor Tapes
2		
3		
4		

Table 5.   Supramolecular Structural Parameters for Piperazinediones **2-7**: Arene Interactions.[a]

| Compound | Within a Tape | | | in Lateral Neighbor Tapes | | | in Vertical Neighbor Tapes | | | and H[c] |
	κ_1 (Å)	ζ_1 (deg)	τ_1 (deg)	κ_2 (Å)	ζ_2 (deg)	τ_2 (deg)	κ_3 (Å)	ζ_3 (deg)	τ_3 (deg)	γ (Å)
2	7.91	nr[d]	12.2	3.82	8.1	12.2	4.99	41.2	0.0	3.79
							5.81	67.4	0.0	
3	6.32	nr	57.2	6.06	53.9	0.00	6.03	61.4	0.0	3.13
4	6.16	42.8	0.0	4.90	14.4	86.3	7.52	69.8	85.6	2.76
	6.16	43.1	0.0	5.56	33.2	85.6	7.75	nr	86.8	3.26
5[e,f]	6.20 H/H	nr	77.1	6.02 H/H	nr	45.8	4.84 H/M	nr	5.5	2.86[g]
	6.22 H/H	nr	77.1	8.62 M/M	nr	39.5	4.87 H/M	nr	5.3	2.93[g]
	5.48 M/M	nr	70.6	7.10 H/M	nr	42.6				2.93[h]
	5.52 M/M	nr	70.6							2.96[h]
6	6.15 H/H	48.1	0.0	4.81 H/H	15.6	83.8	7.29 H/H	nr	83.8	2.58 H/H
	6.15 O/O	47.1	0.0	4.82 O/O	14.3	85.8	8.42 O/O	70.3	0.0	2.64 O/O
							6.30 H/O	nr	25.2	
7	6.06 M/M	50.3	0.0	5.62 M/M	50.7	0.0	6.64 M/O	nr	20.5	2.79[i]
	6.06 O/O	48.9	0.0	5.61 O/O	nr	82.3	7.40 O/O	61.1	0.0	3.28[j]
							7.57 M/M	nr	79.4	

[a]For optimal face-to-face interactions, $\kappa \approx 3.8$ Å, $0° < \zeta < 35°$, and $\tau = 0°$. For optimal edge-to-face interactions, $\kappa \approx 5.0$ Å, $0° < \zeta < 35°$, and $\tau \approx 90°$. [b]H represents an unsubstituted arene, M represents a dimethyl arene, and O represents a dimethoxy arene. [c]Distance from an arene centroid to the nearest hydrogen. [d]Not recorded. [e]Two conformers, **6a** and **6b**, alternate in each hydrogen-bonded tape. [f]Adjacent LNTs and VNTs are enantiomeric; i.e., they are composed of the conformational enantiomers of **6a** and **6b**. [g]Hydrogen of methyl group to centroid of arene of VNT. [h]Hydrogen of unsubstituted arene to VNT. [i]Hydrogen of methoxy group to LNT. [j]Hydrogen of methyl group to LNT.

bonded tape and projection of the other arene ring below this plane alternately for adjacent molecules along the tape, producing a "bow tie" motif seen when a tape is viewed down the hydrogen bonding axis (Table 4). No intratape or intertape arene interactions exist as evidenced by the large centroid–to–centroid distances for adjacent molecules within a tape, in LNTs, and in VNTs ($\kappa > 6$ Å). VNTs are directly stacked. Coupled with the "rocked" orientation of adjacent members in a tape and the folding of the cyclopentene rings, this stacking creates an edge topography that permits interdigitation of the methyl groups of LNTs, which are offset by 3 Å. In this way, van der Waals interactions are maximized and free space is minimized in this crystal.

Tape morphology for piperazinedione 4 is quite different from that of 2 or 3. Tapes are constructed from a single conformer of 4 that lacks rotational, inversion, and mirror symmetry. All molecules in a single hydrogen–bonded tape are related by translation, not by a two–fold rotation or inversion. Therefore, the edges of a tape present different topographies. A "bent H" motif is seen when a tape is viewed down the hydrogen bonding axis (Table 4). No intratape arene face–to–face interactions occur as evidenced by the large centroid–to–centroid distances ($\kappa_1 = 6.16$ Å) and offset angles ($\zeta_1 \approx 47°$) for arenes on edges of the tape, despite the fact that adjacent arene rings are parallel ($\tau_1 = 0$). The folding of the cyclopentene rings toward nitrogen serves to minimize the free volume between indane moieties of adjacent hydrogen–bonded molecules, narrowing the width and compacting the tape, and facilitates LNT interactions by more fully exposing one face of each arene. LNTs are arranged in a "herringbone" motif (see the LNT column of Table 4). The arene centroid–to–centroid distances ($\kappa_2 = 4.90$ Å on one edge and 5.56 Å on the other edge), offset angles ($\zeta_2 = 14.4°$ and 33.2°), tilt angles ($\tau_2 = 86.3°$ and 85.6°), and the distances from the arene centroid to the closest arene hydrogen ($\gamma = 2.76$ Å and 3.26 Å) are consistent with arene edge–to–face interactions (Table 5).[12] Abutment of LNTs, which for 4 are related by screw symmetry, produces sheets with a corrugated topography with identifiable "major" and "minor" grooves and "narrow" and "broad" ridges (Figure 1). Due to the complementarity of the pattern on the opposing sides, these sheets nest in the crystalline solid (see the VNT column of Table 4).
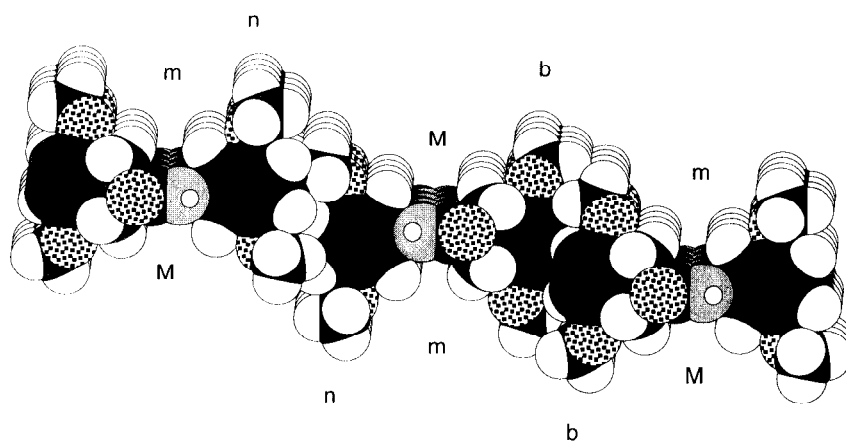

Figure 1. Sheet topography for piperazinedione 4. Labeled features include major grooves (M), minor grooves (m), narrow ridges (n), and broad ridges (b).

For piperazinedione **5**, LNTs and VNTs are enantiomeric: half of the hydrogen–bonded tapes are composed of alternating conformers **5a** and **5b**, while the other half of the tapes are composed of the enantiomers of these conformers. As was the case for piperazinedione **3**, the amide hydrogen bonds are of normal length, but the average planes of adjacent piperazinedione rings are sharply canted (τ_p = 69.2°). In this case the unsubstituted arene rings of conformers **5a** are projected above the average plane of the hydrogen–bonded tape and the unsubstituted arene rings of conformers **5b** are projected below this plane, producing a tape with a trapezoidal cross section when viewed down the hydrogen bonding axis (see the VNT column in Table 4). Both LNTs and VNTs are oriented "head–to–tail". Intratape and LNT intertape arene interactions are absent as evidenced by the large centroid–to–centroid distances, but the arene centroid–to–centroid distances for VNTs (κ_3 = 4.84 and 4.87 Å) and the centroid–to–hydrogen distances (2.86 Å $\le \gamma \le$ 2.96 Å) are consistent with reciprocal van der Waals contacts. These occur between a hydrogen of a methyl substituent and the unsubstituted arene of the VNT and between a hydrogen of the unsubstituted arene and the methyl–substituted arene of the VNT. Similar to **3**, LNTs of **5** have an edge topography that permits shallow interdigitation of hydrogens, maximizing van der Waals interactions and minimizing free space in this crystal.

Tape morphology for piperazinedione **6** is similar to that of **4**. Tapes are constructed from a single conformer of **6** that lacks molecular mirror symmetry. All molecules in a hydrogen–bonded tape are related by translation, and so the edges of a tape necessarily present different topographies. A "bent T" motif is seen when a tape is viewed down the hydrogen bonding axis (Table 4). No intratape arene face–to–face interactions occur as evidenced by the large centroid–to–centroid distances (κ_1 > 6 Å) and offset angles (ζ_1 > 47°) for arenes on edges of the tape, despite the fact that adjacent arene rings are parallel. The folding of the cyclopentene rings facilitates arene interactions between LNTs which are arranged in a "herringbone" motif in a "head–to–head, tail–to–tail" fashion (Table 4). The arene centroid–to–centroid distances (κ_2 = 4.81 Å on the unsubstituted arene edge and 4.82 Å on the methoxy–substituted arene edge), offset angles (ζ_2 = 15.6° and 14.3°), tilt angles (τ_2 = 83.8° and 85.8°), and the distances from the arene centroid to the closest arene hydrogen (γ = 2.58 Å and 2.64 Å) are all consistent with arene edge–to–face interactions.[12] Abutment of LNTs, which are related by screw symmetry, produces sheets with a regular corrugated topography that nest in the crystal (Table 4).

Tape morphology for piperazinedione **7** resembles that of **6**. Tapes are constructed from one conformer of **7** that lacks molecular mirror symmetry. All molecules in a hydrogen–bonded tape are related by translation, and so the edges of a tape necessarily present different topographies. A "bent T" motif is seen when a tape is viewed down the hydrogen bonding axis (Table 4). LNTs are are arranged in a "head–to–head, tail–to–tail" fashion. However, enantiomeric conformers co–occur in the crystal and give rise to enantiomeric hydrogen–bonded tapes. The repeat pattern in the crystal viewed down the hydrogen–bonded tape axis is

....B–A A–B B'–A' A'–B'....
....A–B B'–A' A'–B' B–A....
....B'–A' A'–B' B–A A–B....
....A'–B' B–A A–B B'–A'....
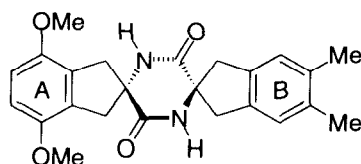
7 = A–B
ent-7 = A'–B'
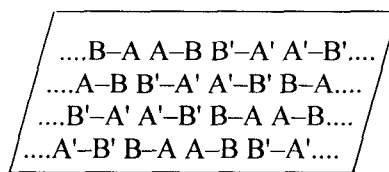
In the case of **7** accomodation of the methyl substituents results in greater spacing of the LNTs. The methyl substituents of LNTs, which are rotationally disordered in the crystal, are abutted edge–to–edge (Table 4). Although dimethylarene moieties of LNTs are parallel, intertape face–to–face arene interactions do not occur as evidenced by the large centroid–to–centroid distance ($\kappa_2 = 5.62$ Å) and offset angle ($\zeta_2 = 50.7°$). The distance from the dimethylarene centroid to a hydrogen of a methyl group of the LNT is about 3.8 Å. On the opposite edge, the dimethoxyarene moieties are aranged in a "herringbone" motif. However, intertape edge–to–face arene interactions do not occur as evidenced by the large centroid–to–centroid distance ($\kappa_2 = 5.61$ Å). Rather, the distance from the dimethoxyarene centroid to a hydrogen of a methoxy group of the LNT is 2.79 Å. As was the case for **4** and **6**, abutment of LNTs produces sheets with a regular corrugated topography that nest in the crystalline solid.

DISCUSSION

We postulated that predictable molecular order in crystalline solids would arise if chiral molecular building blocks were to contain three linearly independent recognition elements.[6b] Our design model envisaged that molecules **1**, built from enantiomerically pure derivatives of 2–aminoindan–2–carboxylic acid, would provide a suitable conformationally restricted, directed molecular scaffold for the required recognition elements. We have established that symmetrical and unsymmetrical piperazinediones **1** can easily be prepared from 2–aminoindan–2–carboxylic acid derivatives, which are in turn synthesized from ethyl glycinate and substituted *o*–xylene dibromides. The first intermolecular recognition element, amide–to–amide hydrogen bonding of the piperazinedione ring, was operative in each of our prototype piperazinediones **2–7**. It seems likely that "ladder–like" hydrogen–bonded tapes will form for type **1** piperazinediones irrespective of the groups R^1–R^8. In light of the solid state structures of the piperazinediones documented in the CSD and reported elsewhere,[4–6] it was surprising that a variety of tape structural motifs, involving boat, planar, or even chair conformers of the piperazinedione ring, and coplanar to sharply canted orientations of neighboring piperazinedione rings in the tape, occured for piperazinediones **2–7** in the solid state. This conformational and orientational flexibility bodes well for future attempts to engineer interactions between groups R^1–R^8 that involve interactions stronger than van der Waals contacts.

We anticipated that, in the absence of groups R^1–R^8, intermolecular arene interactions perpendicular to the hydrogen–bonded tapes would contribute to the establishment of order in the crystal. In fact, parallel–displaced arene pairs were observed for LNTs in the butterfly motif of **2**. Sheets formed from LNTs of **2** had a dimpled topography that facilitated van der Waals contacts between adjacent sheets in the solid. Our first structural modifications involved attachment of methoxy and methyl arene substituents which were incompatible with the crystal packing observed for **2**. Edge–to–face arrays were seen in the herringbone motifs of LNTs of methoxy–substituted piperazinediones **4** and **6**. Sheets formed from LNTs of **4** and **6** had corrugated topopographies which again maximized van der Waals contacts between adjacent sheets in the solid. Arene edge–to–face interactions were precluded by methyl substitution on one edge only for piperazinediones **5** and **7** and on both edges for piperazinedione **3**. In the case of **7**, the head–to–tail arrangement of LNTs led to a "doublewide" herringbone motif and to crystal packing similar to that observed for **4** and **6**. Piperazinediones **3** and **5** exhibited novel tape morphologies that lacked arene interactions between LNTs, but exposed arene faces

to contacts with hydrogens of VNTs. Van der Waals contacts between LNTs were maximized by shallow interdigitation of the edges of the tapes.

Having demonstrated the reliability and flexibility of hydrogen–bonded "ladder–like" tape formation for achiral piperazinediones 1, the next structural modification involved placement of functionality on the arene rings to establish a dipole orthogonal to the tape axis. This work is described in the accompanying article in this issue.[6d]

EXPERIMENTAL

General Procedures

All reactions were performed under a positive pressure of argon. Moisture sensitive reactions were performed in glassware flame–dried under vacuum immediately before use. Reaction mixtures were stirred magnetically. Hygroscopic liquids were transferred via syringe and were introduced into reaction vessels through rubber septa. Reaction product solutions were concentrated using a rotary evaporator at 30–150 mm Hg. Dichloromethane (CH_2Cl_2) and dimethyl sulfoxide (DMSO) were distilled from CaH_2, tetrahydrofuran (THF) was distilled from sodium/benzophenone ketyl, N,N–dimethyl formamide (DMF) was distilled from $MgSO_4$ under reduced pressure, and triethylamine was distilled from and stored over NaOH pellets. Analytical thin–layer chromatography was performed on Merck glass–backed, pre–coated plates (0.25 mm, silica gel 60, F–254). Visualization of spots was effected by dipping the plate in either a 2.5% solution of anisaldehyde in ethanol containing 6% H_2SO_4 and 2% acetic acid or a 5% solution of phosphomolybdic acid in ethanol, followed by charring on a hot plate. Flash chromatography was performed using Merck silica gel 60 (230–400 mesh). Gravity chromatography was performed using Merck silica gel 60 (70–230 mesh). Melting points are uncorrected. Proton and ^{13}C magnetic resonance spectra were recorded at 300, 250, or 200 MHz and 75, 63, or 50 MHz, respectively. Proton NMR spectra were referenced to tetramethylsilane (0 ppm), the residual proton signal of $CDCl_3$ (7.24 ppm), the residual proton signal of TFA–d (11.5 ppm), or the center line of the residual proton signal of DMSO–d_6 (2.49 ppm). Carbon NMR spectra were referenced to the $CDCl_3$ signal (77.0 ppm), TFA–d signal (164.4 ppm), or the DMSO–d_6 signal (39.5 ppm). Mass spectra were obtained from the Mass Spectrometry Lab in the Department of Chemistry at The University of Arizona, Tucson, Arizona. Elemental analyses were performed by Desert Analytics, Tucson, AZ.

Ethyl 2–Aminoindan–2–carboxylate (8a).[8] To a solution of ethyl N–(diphenylmethylene)–glycinate[13] (2.40 g, 9.00 mmol) in THF (110 mL) at –78 °C was added sodium bis(trimethylsilyl)amide (11 mL of 1.0 M solution in THF) in one portion. After 1 h, α,α'–dibromo–o–xylene[14] (2.64 g, 10.0 mmol) in THF (110 mL cooled to –78 °C) was added in one portion. The reaction mixture was stirred for 1 h and warmed to 0 °C. After 24 h, the solution was cooled to –78 °C and additional sodium bis(trimethylsilyl)amide (11 mL of 1.0 M solution in THF) was added. The reaction mixture was stirred for 1 h and warmed to –20 °C. After an additional 24 h, the reaction was allowed to warm to room temperature. The reaction was quenched by cautious addition of brine (200 mL) followed by extraction with EtOAc (3 x 200 mL). The organic extracts were combined, dried ($MgSO_4$), filtered, and concentrated to give a brown oil (3.40 g). The oil was taken up in THF (20 mL), water (1 mL) and TFA (2 mL) were added, and the solution was stirred vigorously. After 1 h, the mixture was diluted with THF (50 mL) and extracted with 2 M NaOH (20 mL) followed by water (20 mL). The organic layer was

dried ($MgSO_4$), filtered, and concentrated to give a red oil. Flash chromatography (50–100% EtOAc/hexanes) afforded 1.36 g (6.6 mmol, 73%) of **8a**, R_f 0.08 (20% EtOAc/hexanes) as a clear, yellow oil. ^{1}H NMR ($CDCl_3$) δ 1.27 (3, t, J = 9.0 Hz), 1.80 (2, s), 2.84 (2, d, J = 16 Hz), 3.54 (2, d, J = 16 Hz), 4.20 (2, q, J = 9.0 Hz), 7.17 (4, m); ^{13}C NMR ($CDCl_3$) δ 13.9, 45.9, 60.9, 64.6, 124.5, 126.5, 140.2, 176.2.

Ethyl 2-Amino-5,6-dimethylindan-2-carboxylate (8b).[8] By a similar procedure, **8b** was prepared from ethyl *N*-(diphenylmethylene)glycinate (2.40 g, 9.00 mmol) and 1,2-bis(chloromethyl)-4,5-dimethylbenzene[14] (2.03 g, 10.0 mmol). Flash chromatography (50–100% EtOAc/hexanes) afforded 1.43 g (6.1 mmol, 68%) of **8b**, R_f 0.10 (20% EtOAc/hexanes) as a clear, yellow oil. ^{1}H NMR ($CDCl_3$) δ 1.27 (3, t, J = 7.0 Hz), 1.87 (2, s), 2.21 (6, s), 2.78 (2, d, J = 16.0 Hz), 3.48 (2, d, J = 16.0 Hz), 4.19 (2, q, J = 7.0 Hz), 6.97 (2, s); ^{13}C NMR ($CDCl_3$) δ 14.7, 20.3, 46.4, 61.7, 65.7, 126.4, 135.4, 138.5, 177.1.

Ethyl 2-Amino-4,7-dimethoxyindan-2-carboxylate (8c).[8] To a solution of ethyl *N*-(phenylmethylene)glycinate[15] (1.91 g, 10.0 mmol) in THF (100 mL) at –78 °C was added NaHMDS (22 mL of 1.0 M solution in THF, 22 mmol) in one portion. After 45 min, 2,3-bis(bromomethyl)-1,4-dimethoxybenzene[16] (3.24 g, 10.0 mmol) in THF (100 mL) was added in one portion. The reaction mixture was removed from the cooling bath and allowed to warm to room temperature. After 2 h, the reaction was quenched by addition of water (500 mL) followed by extraction with EtOAc (3 x 500 mL). The organic extracts were combined, dried ($MgSO_4$), filtered, and concentrated to give a red oil (3.40 g). The oil was suspended in ether (10 mL) and 2 M HCl (10 mL) and the mixture was stirred vigorously. After 2 h, the layers were separated and the organic layer was washed with water (10 mL). The aqueous phase and wash were combined, neutralized with $NaHCO_3$, and extracted with $CHCl_3$ (3 x 15 mL). The organic extracts were combined, dried ($MgSO_4$), filtered, and concentrated to give a light yellow oil. Flash chromatography (5% methanol/ CH_2Cl_2) afforded 928 mg (3.5 mmol, 35%) of **8c**, R_f 0.60 (10% methanol/ CH_2Cl_2) as a clear, colorless oil. ^{1}H NMR ($CDCl_3$) δ 1.24 (3, t, J = 7.1 Hz), 1.96 (2, br s), 2.88 (2, d, J = 16.2 Hz), 3.42 (2, d, J = 16.2 Hz), 3.74 (6, s), 4.18 (2, q, J = 7.1 Hz), 6.62 (2, s); ^{13}C NMR ($CDCl_3$) δ 14.1, 43.5, 55.5, 61.2, 64.6, 109.1, 129.8, 150.3, 176.4.

2-[(N-Carbo-2,2-dimethylethoxy)amino]indan-2-carboxylic Acid (9a). To a solution of **8a** (230 mg, 0.87 mmol), $NaHCO_3$ (79 mg, 0.94 mmol) and NaCl (230 mg, 3.9 mmol) in water (2.5 mL) and CH_2Cl_2 (2.5 mL) was added di-*t*-butyl dicarbonate (248 mg, 1.14 mmol). The resultant biphasic mixture was heated to reflux. After 2 h, the mixture was cooled to room temperature, the organic layer was removed, and the aqueous layer was extracted with $CHCl_3$ (3 x 3.5 mL). The organic extracts were combined, dried ($MgSO_4$), filtered, and concentrated to give a light yellow oil. Flash chromatography (30% EtOAc/hexanes) afforded 285 mg (0.781 mmol, 90%) of ethyl 2-[(*N*-carbo-2,2-dimethylethoxy)amino]indan-2-carboxylate, R_f 0.35 (30% EtOAc/hexanes) as a white solid, mp 143–144 °C. IR cm^{-1} 3330, 1730, 1705; ^{1}H NMR ($CDCl_3$) δ 1.26 (3, t, J = 7.1 Hz), 1.42 (9, s), 3.20 (2, d, J = 16.5 Hz), 3.65 (2, d, J = 16.5 Hz), 4.22 (2, q, J = 7.1 Hz), 5.06 (1, br s), 7.19 (4, m); ^{13}C NMR ($CDCl_3$) δ 14.2, 28.3, 43.9, 61.5, 66.0, 80.0, 124.6, 127.0, 139.8, 155.0, 173.5.

To a solution of ethyl 2-[(*N*-carbo-2,2-dimethylethoxy)amino]indan-2-carboxylate (300 mg, 1.03 mmol) in water (3.0 mL) and methanol (18.0 mL) was added 2 M NaOH (1 mL, 2 mmol). After stirring at room temperature for 24 h, the solution was concentrated to 5 mL, diluted with water (5 mL), and treated with

2 M HCl to produce a solution acidic by pH paper. The aqueous mixture was extracted with Et_2O (3 x 20 mL). The organic extracts were combined, dried ($MgSO_4$), filtered, and concentrated to give 266 mg (0.955 mmol, 93%) of **9a**, R_f 0.30 (10% methanol/CH_2Cl_2), as a white solid, mp 170–172 °C (dec). IR cm^{-1} 3380, 3300–2800 (br), 1760, 1675, 1525; ^{1}H NMR ($CDCl_3$) δ 1.39 (9, s), 3.26 (2, d, J = 16.5 Hz), 3.66 (2, d, J = 16.5 Hz), 5.12 (1, br s), 7.18 (4, m); ^{13}C NMR ($CDCl_3$) δ 28.2, 43.9, 65.7, 80.6, 124.5, 127.0, 139.6, 155.7, 178.5.

Anal. Calcd for $C_{15}H_{19}NO_4$: C, 64.97; H, 6.91. Found: C, 64.54; H, 6.63.

2-[(N–Carbo–2,2–dimethylethoxy)amino]–5,6–dimethylindan–2–carboxylic Acid (9b). By a similar procedure, **8b** (1.11 g, 4.74 mmol) afforded 1.30 g (3.9 mmol, 82%) of ethyl 5,6–dimethyl–2–[(N–carbo–2,2–dimethylethoxy)–amino]indan–2–carboxylate, R_f 0.40 (20% EtOAc/hexanes) as a clear, colorless oil. IR cm^{-1} 3395, 1740, 1720; ^{1}H NMR ($CDCl_3$) δ 1.25 (3, t, J = 7.0 Hz), 1.41 (9, s), 2.21 (6,s), 3.11 (2, d, J = 16.4 Hz), 3.56 (2, d, J = 16.4 Hz), 4.20 (2, q, J = 7.0 Hz), 5.23 (1, br s), 6.96 (2, s); ^{13}C NMR ($CDCl_3$) δ 13.9, 19.5, 28.0, 43.4, 61.2, 66.0, 79.5, 125.4, 134.9, 137.2, 154.9, 173.4.

Ethyl 2–[(N–carbo–2,2–dimethylethoxy)amino]–5,6–dimethylindan–2–carboxylate (504 mg, 1.51 mmol) was similarly hydrolyzed to afford 460 mg (1.51 mmol, 99%) of **9b**, R_f 0.36 (10% methanol/CH_2Cl_2), as a white solid, mp 268–270 °C (dec). IR cm^{-1} 3400–2500 (br), 3300, 3250, 1720, 1650; ^{1}H NMR (acetone-d_6) δ 1.37 (9, s), 2.18 (6, s), 3.22 (2, d, J = 16.0 Hz), 3.51 (2, d, J = 16.0 Hz), 6.51 (1, br s), 6.93 (2, s); ^{13}C NMR (acetone-d_6) δ 19.6, 28.5, 43.8, 66.6, 79.1, 126.2, 135.3, 138.8, 156.1, 175.3.

2-[(N–carbo–2,2–dimethylethoxy)amino]–4,7–dimethoxyindan–2–carboxylic Acid (9c). By a similar procedure, **8c** (230 mg, 0.87 mmol) afforded 285 mg (0.781 mmol, 90%) of ethyl 4,7–dimethoxy–2–[(N–carbo–2,2–dimethyl–ethoxy)amino]indan–2–carboxylate, R_f 0.35 (30% EtOAc/hexanes) as a white solid, mp 150–153 °C. IR cm^{-1} 3370, 1710, 1740; ^{1}H NMR ($CDCl_3$) δ 1.25 (3, t, J = 9.0 Hz), 1.41 (9, s), 3.18 (2, d, J = 17.9 Hz), 3.56 (2, d, J = 17.9 Hz), 3.78 (6, s), 4.21 (2, q, J = 9.0 Hz), 5.12 (1, br s), 6.64 (2, s); ^{13}C NMR ($CDCl_3$) δ 14.1, 28.2, 41.8, 55.8, 61.5, 65.8, 80.0, 109.1, 129.1, 150.0, 154.9, 173.6.

Ethyl 2–[(N–carbo–2,2–dimethylethoxy)amino]–4,7–dimethoxyindan–2–carboxylate (307 mg, 0.84 mmol) was similarly hydrolyzed to afford 270 mg (0.80 mmol, 95%) of **9c**, R_f 0.36 (10% methanol/CH_2Cl_2), as a white solid, mp 261–263 °C (dec). IR cm^{-1} 3400–2600 (br), 3340, 1720, 1650; ^{1}H NMR ($CDCl_3$) δ 1.40 (9, s), 3.21 (2, d, J = 17.8 Hz), 3.61 (2, d, J = 17.8 Hz), 3.78 (6, s), 5.19 (1, br s), 6.64 (2, s); ^{13}C NMR ($CDCl_3$) δ 28.1, 29.3, 41.4, 55.6, 65.8, 81.0, 109.2, 129.5, 150.4, 155.5.

Anal. Calcd for $C_{17}H_{23}NO_6$: C, 60.52; H, 6.87. Found: C, 61.12; H, 7.08.

N–[2–(Carboethoxy)indan–2–yl]–2–[(N–carbo–2,2–dimethylethoxy)amino]indan–2–carboxamide (10a). To a solution of **8a** (483 mg, 1.82 mmol), **9a** (483 mg, 1.43 mmol), and triethylamine (300 μL) in DMF (7.25 mL) was added BOP reagent[17] (632 mg, 1.43 mmol). After stirring at room temperature for 24 h, the solution was diluted with EtOAc (50 mL) and water (25 mL). The organic layer was removed and the aqueous layer was extracted with EtOAc (2 x 50 mL). The organic extracts were combined and sequentially washed with 3 M HCl (2 x 50 mL), water (50 mL), saturated $NaHCO_3$ (2 x 50 mL), water (50 mL), then dried ($MgSO_4$), filtered, and concentrated to give a light yellow solid. Recrystallization from EtOAc/hexanes (1:3) afforded 685 mg (1.17 mmol, 82%) of **10a**, R_f 0.40 (46% EtOAc/hexanes), as a white solid, mp 200–203 °C. IR cm^{-1} 3350, 3280, 1745, 1690, 1660; ^{1}H NMR ($CDCl_3$) δ 1.20 (3, t, J = 8.0 Hz), 1.23 (9, s), 3.25 (4, d, J = 16.0 Hz), 3.64 (4, d, J

= 16.0 Hz), 4.16 (2, q, J = 8.0 Hz), 5.22 (1, br s), 7.14 (8, m), 7.23 (1, br s); ^{13}C NMR (CDCl$_3$) δ 14.0, 27.9, 42.5, 43.3, 61.4, 65.7, 66.7, 80.1, 124.4, 124.6, 124.7, 126.7, 126.8, 139.7, 154.8, 172.9, 173.0.

Anal. Calcd for C$_{27}$H$_{32}$N$_2$O$_5$: C, 69.81; H, 6.94. Found: C, 69.38; H, 7.05.

5,6–Dimethyl–N–[5,6–dimethyl–2–(carboethoxy)indan–2–yl]–2–[(N–carbo–2,2–dimethylethoxy)amino]indan–2–carboxamide (10b). By a similar procedure, **8b** (782 mg, 2.26 mmol) and **9b** (460 mg, 1.51 mmol) were coupled to give 650 mg (1.25 mmol, 83%) of **10b**, R$_f$ 0.20 (20% EtOAc/hexanes), as a white solid, mp 187–188 °C. IR cm^{-1} 3365, 3280, 1740, 1685, 1660; ^{1}H NMR (CDCl$_3$) δ 1.20 (3, t, J = 7.6 Hz), 1.21 (9, s), 2.18 (6, s), 2.19 (6, s), 3.12 (4, d, J = 16.2 Hz), 3.56 (4, d, J = 16.2 Hz), 4.16 (2, q, J = 7.6 Hz), 5.05 (1, br s), 6.93 (4, s), 7.20 (1, br s); ^{13}C NMR (CDCl$_3$) δ 14.1, 19.6, 19.7, 27.9, 42.4, 43.2, 61.3, 65.9, 67.0, 80.3, 125.6, 125.7, 134.9, 135.1, 137.2, 137.3, 154.8, 172.9.

4,7–Dimethoxy–N–[4,7–dimethoxy–2–(carboethoxy)indan–2–yl]–2–[(N–carbo–2,2–dimethylethoxy)amino]–indan–2–carboxamide (10c). By a similar procedure, **8c** (483 mg, 1.82 mmol) and **9c** (483 mg, 1.43 mmol) were coupled to give 685 mg (1.17 mmol, 82%) of **10c**, R$_f$ 0.40 (46% EtOAc/hexanes), as a white solid, mp 200–203 °C. IR cm^{-1} 3440, 3320, 1745, 1705, 1660; ^{1}H NMR (CDCl$_3$) δ 1.22 (3, t, J = 8.6 Hz), 1.28 (9, s), 3.22 (4, d, J = 18.0 Hz), 3.54 (4, d, J = 18.0 Hz), 3.78 (12, s), 4.21 (2, q, J = 8.6 Hz), 5.24 (1, br s), 6.59 (2, s), 6.63 (2, s), 7.10 (1, br s); ^{13}C NMR (acetone-d_6) δ 14.3, 28.2, 41.2, 41.6, 55.7, 60.4, 61.5, 66.0, 67.0, 109.8, 109.9, 129.1, 130.3, 130.6, 155.6, 173.8.

Anal. Calcd for C$_{31}$H$_{40}$N$_2$O$_9$: C, 63.69; H, 6.90. Found: C, 63.75; H, 7.18.

N–[5,6–Dimethyl–2–(carboethoxy)indan–2–yl]–2–[(N–carbo–2,2–dimethylethoxy)amino]indan–2–carboxamide (10d). By a similar procedure, **8a** (260 mg, 1.27 mmol) and **9b** (300 mg, 0.98 mmol) were coupled to give 400 mg (0.81 mmol, 83%) of **10d**, R$_f$ 0.27 (20% EtOAc/hexanes). Recrystallization from 60% EtOAc/hexanes gave colorless crystals, mp 186–188 °C. IR cm^{-1} 3394, 3299, 1727, 1714, 1665; ^{1}H NMR (CDCl$_3$) δ 1.23 (12, m), 2.21 (6, s), 3.24 (4, d, J = 16.7 Hz), 3.60 (4, m), 4.19 (2, q, J = 7 Hz), 5.09 (1, br s), 6.94 (2, s), 7.16 (4, s); ^{13}C NMR (CDCl$_3$) δ 14.6, 20.2, 28.5, 43.0, 43.9, 61.9, 66.2, 67.5, 80.8, 125.0, 126.2, 127.3, 135.7, 137.8, 140.3, 155.3, 173.3, 173.5.

Anal. Calcd. for C$_{29}$H$_{36}$N$_2$O$_5$: C, 70.73; H, 6.90; N, 5.69. Found: C, 70.54; H, 7.12; N, 5.58.

N–[4,7–Dimethoxy–2–(carboethoxy)indan–2–yl]–2–[(N–carbo–2,2–dimethylethoxy)amino]indan–2–carboxamide (10e). By a similar procedure, **8a** (782 mg, 2.26 mmol) and **9c** (460 mg, 1.51 mmol) were coupled to give 650 mg (1.25 mmol, 74%) of **10e**, R$_f$ 0.20 (20% EtOAc/hexanes), as a white solid, mp 189–191 °C. IR cm^{-1} 3370, 3280, 1720, 1700, 1680; ^{1}H NMR (CDCl$_3$) δ 1.21 (3, t, J = 7.0 Hz), 1.28 (9, s), 3.24 (4, d, J = 16.5 Hz), 3.56 (4, d, J = 16.5 Hz), 3.74 (6, s), 4.18 (2, q, J = 7.0 Hz), 5.18 (1, br s), 6.59 (2, s), 7.16 (4, s), 7.28 (1, s); ^{13}C NMR (CDCl$_3$) δ 14.1, 27.9, 41.2, 42.6, 55.5, 61.5, 65.3, 66.8, 80.2, 109.2, 124.7, 126.9, 129.3, 139.9, 150.0, 154.9, 172.8, 172.9; HRMS (FAB$^+$) calcd for C$_{29}$H$_{37}$N$_2$O$_7$ (M + H$^+$) 525.2601, found 525.2601.

N–[5,6–Dimethyl–2–(carboethoxy)indan–2–yl]–2–[(N–carbo–2,2–dimethylethoxy)amino]–4,7–dimethoxyindan–2–carboxamide (10f). By a similar procedure, **8c** (300 mg, 1.13 mmol) and **9b** (300 mg, 0.98 mmol) were coupled to give 450 mg (0.83 mmol, 84%) of **10f**, R$_f$ 0.25 (20% EtOAc/hexanes). Recrystallization from EtOAc

gave colorless crystals, mp 194–197 °C. IR cm^{-1} 3371, 3329, 1724, 1716, 1666; ^{1}H NMR (CDCl$_3$) δ 1.28 (12, m), 2.21 (6, s), 3.23 (4, d, J = 17.0 Hz), 3.56 (4, d, J = 17.2 Hz), 3.75 (6, s), 4.18 (2, q, J = 7 Hz), 5.18 (1, br s), 6.60 (2, s), 6.95 (2, s); ^{13}C NMR (CDCl$_3$) δ 14.6, 20.2, 28.4, 41.7, 44.0, 56.0, 61.9, 65.8, 67.5, 80.5, 109.7, 126.2, 129.9, 135.6, 137.8, 150.5, 155.3, 173.4.

Anal. Calcd. for C$_{31}$H$_{40}$N$_2$O$_7$: C, 67.39; H, 7.24; N, 5.07. Found: C, 67.01; H, 7.40; N, 4.81.

Cyclo–bis(2–Aminoindan–2–carboxylic Acid) (2). A sample of **10a** (106 mg, 0.18 mmol) was heated in a sealed, evacuated tube for 30 min at 240–245 °C in an oil bath. The sample melted, evolved gas, and resolidified. After cooling to room temperature, the solid was recrystallized from TFA/DMSO to give 74.7 mg (0.17 mmol, 95%) of **2** as a white solid, mp 322–324 °C. IR cm^{-1} 3180, 1680; ^{1}H NMR (TFA–d) δ 3.26 (4, d, J = 16.0 Hz), 3.86 (4, d, J = 16.0 Hz), 7.15 (8, m); ^{13}C NMR (TFA–d) δ 48.6, 68.9, 126.7, 130.3, 139.2, 175.2.

Anal. Calcd for C$_{20}$H$_{18}$N$_2$O$_2$: C, 75.45; H, 5.70; N, 8.80. Found: C, 75.12; H, 5.44; N, 8.70.

Cyclo–bis(2–Amino–5,6–dimethylindan–2–carboxylic Acid) (3). By a similar procedure, **10b** (45.8 mg, 0.088 mmol) gave 27.1 mg (0.072 mmol, 82%) of **3** as a white solid, mp >400 °C, after recrystallization from TFA/DMSO. IR cm^{-1} 3170, 1680; ^{1}H NMR (TFA–d) δ 2.14 (12, s) 3.19 (4, d, J = 16.5 Hz), 3.78 (4, d, J = 16.5 Hz), 6.91 (4, s); ^{13}C NMR (TFA–d) δ 20.1,48.3, 68.8, 127.5, 136.6, 139.5, 176.1.

Anal. Calcd for C$_{24}$H$_{26}$N$_2$O$_2$: C, 76.78; H, 7.00; N, 7.48. Found: C, 76.98; H, 7.29; N, 7.22.

Cyclo–bis(2–Amino–4,7–dimethoxyindan–2–carboxylic Acid) (4). By a similar procedure, **10c** (106 mg, 0.18 mmol) gave 74.7 mg (0.17 mmol, 95%) of **3** as a white solid, mp >300 °C, after recrystallization from DMSO. IR cm^{-1} 3170, 1680; ^{1}H NMR (DMSO–d$_6$) δ 3.02 (4, d, J = 18.0 Hz), 3.46 (4, d, J = 18.0 Hz), 3.74 (12, s), 6.74 (4, s), 8.70 (2, s); ^{13}C NMR (DMSO–d$_6$) δ 44.0, 54.2, 63.2, 109.1, 129.1, 149.2, 170.8.

Anal. Calcd for C$_{24}$H$_{26}$N$_2$O$_6$: C, 65.74; H, 5.89; N, 6.39. Found: C, 65.87; H, 6.12; N, 6.37.

Cyclo[(2–Amino–5,6–dimethylindan–2–carboxylic Acid) (2–Aminoindan–2–carboxylic Acid)] (5). By a similar procedure, **10d** (100 mg, 0.20 mmol) gave 50 mg (0.14 mmol, 71%) of **5** as a white solid, mp 316–318 °C, after recrystallization from DMSO. IR cm^{-1} 3170, 3037, 2938, 1666, 1426; ^{1}H NMR (TFA–d) δ 2.18 (6, s) 3.22 (2, d, J = 13.7 Hz), 3.30 (2, d, J = 13.4 Hz), 3.85 (4, app t), 6.95 (2, s), 7.19 (4, s); ^{13}C NMR (TFA–d) δ 20.5, 48.7, 48.9, 69.1, 69.2, 127.0, 127.9, 130.6, 137.0, 139.5, 139.8, 175.4, 175.8.

Anal. Calcd. for C$_{22}$H$_{22}$N$_2$O$_2$: C, 76.30; H, 6.35; N, 8.09. Found: C, 76.39; H, 6.46; N, 8.10.

Cyclo[(2–Amino–4,7–dimethoxyindan–2–carboxylic Acid) (2–Aminoindan–2–carboxylic Acid)] (6). By a similar procedure, **10e** (100 mg, 0.19 mmol) gave 55 mg (0.15 mmol, 76%) of **6** as a white solid, mp 311–312 °C, after recrystallization from DMSO. IR cm^{-1} 3180, 2947, 1677; ^{1}H NMR (TFA–d) δ 3.37 (2, d, J = 16.5 Hz), 3.46 (2, d, J = 17.1 Hz), 3.96 (10, br s), 6.98 (2, s), 7.26 (4, s); ^{13}C NMR (TFA–d) δ 46.0, 48.6, 58.9, 68.7, 68.9, 116.0, 126.8, 130.3, 130.4, 139.3, 152.4, 174.8, 175.3; HRMS (FAB+) calcd for C$_{22}$H$_{23}$N$_2$O$_4$ 379.1658, found 379.1658.

Cyclo[(2–Amino–4,7–dimethoxyindan–2–carboxylic Acid) (2–Amino–5,6–dimethylindan–2–carboxylic Acid)] *(7)*. By a similar procedure, **10f** (135 mg, 0.24 mmol) gave 63 mg (0.15 mmol, 64%) of **7** as a white solid, mp 344–346 °C, after recrystallization from DMSO. IR cm^{-1} 3040, 2950, 1669, 1494; ^{1}H NMR (TFA–*d*) δ 2.20 (6, s) 3.26 (2, d, J = 16.5 Hz), 3.41 (2, d, J = 16.8 Hz), 3.80–3.92 (10, m), 6.94–6.98 (4, m); ^{13}C NMR (TFA–*d*) δ 20.4, 46.0, 48.5, 59.0, 68.7, 69.1, 119.2, 127.8, 130.5, 136.8, 139.6, 152.4, 174.8, 175.8.

Anal. Calcd. for $C_{24}H_{26}N_2O_4$: C, 70.93; H, 6.40; N, 6.89. Found: C, 70.57; H, 6.50; N, 6.72.

ACKNOWLEDGMENT

REFERENCES

1. (a) Pauling, L. *The Nature of the Chemical Bond and the Structure of Molecules and Crystals*, 3rd Ed.; Cornell University Press: Ithaca, NY, 1960. (b) Kitaigorodsky, A. I. *Molecular Crystals and Molecules* ; Academic Press: New York, 1973. (c) Desiraju, G. R. *Crystal Engineering: The Design of Organic Solids* ; Elsevier: Amsterdam, 1989. (d) Wright, J. D. *Molecular Crystals*, 2nd Ed.; Cambridge University Press: Cambridge, England, 1995. (e) MacDonald, J. C.; Whitesides, G. M. *Chem. Rev.* **1994**, *94*, 2383–2420. (f) Lawrence, D. S.; Jiang, T.; Levett, M. *Chem. Rev.* **1995**, *95*, 2229–2260. (g) Lehn, J.–M. *Supramolecular Chemistry* ; VCH: Weinheim, Germany, 1995. (h) *The Crystal as a Supramolecular Entity*, G. R. Desiraju, Ed.; John Wiley & Sons, Ltd: Chichester, England, 1996.

2. Sarma, J. A. R. P.; Desiraju, G. R. *Acc. Chem. Res.* **1986**, *19*, 222–228 and references cited therein.

3. Whitesides, G. M.; Simanek, E. E.; Mathias, J. P.; Seto, C. T.; Chin, D. N.; Mammen, M.; Gordon, D. M. *Acc. Chem. Res.* **1995**, *28*, 37–44 and references cited therein.

4. (a) Corey, R. B. *J. Am. Chem. Soc.* **1938**, *60*, 1598–1604. (b) Degeilh, R.; Marsh, R. E. *Acta Crystallogr.* **1959**, *12*, 1007–1014.

5. (a) Brienne, M–J.; Gabard, J.; Leclercq, M.; Lehn, J.–M.; Cesario, M.; Pascard, C.; Chevé, M.; Dutruc–Rosset, G. *Tetrahedron Lett.* **1994**, *35*, 8157–8160. (b) Palacin, S.; Chin, D. N.; Simanek, E. E.; MacDonald, J. C.; Whitesides, G. M.; McBride, M. T.; Palmore, G. T. R. *J. Am. Chem. Soc.* **1997**, *119*,

11807–11816. (c) Palmore, G. T. R.; McBride, M. T. *Chem. Commun.* **1998**, *119*, 145–146. (d) Chin, D. N.; Palmore, G. T. R.; Whitesides, G. M. *J. Am. Chem. Soc.* **1999**, *121*, 2115–2122.

6. (a) Mash, E. A.; Williams, L. J. *Polym. Preprints* **1996**, *37*, 207. (b) Williams, L. J. Ph.D. Dissertation, The University of Arizona, Tucson, AZ, 1996. (c) Lyon, S. R. Ph.D. Dissertation, The University of Arizona, Tucson, AZ, 1993. (d) Williams, L. J.; Jagadish, B.; Lansdown, M. G.; Carducci, M. D.; Mash, E. A. *Tetrahedron*, article following in this issue.

7. (a) *Nonlinear Optical Properties of Organic Molecules and Crystals*; Academic Press: Orlando, 1987. (b) Prasad, P. N.; Williams, D. J. *Introduction to Nonlinear Optical Effects in Molecules and Polymers;* Wiley–Interscience: New York, 1991. (c) *Nonlinear Optical Materials*; CRC Press: Boca Raton, 1992. (d) *Nonlinear Optics of Organic Molecules and Polymers*; CRC Press: Boca Raton, 1997.

8. Kotha, S.; Kuki, A. *Tetrahedron Lett.* **1992**, *33*, 1565–1568.

9. IUPAC–IUB Commission on Biochemical Nomenclature, *Biochemistry* **1970**, *9*, 3471–3479.

10. Allen, F. H.; Kennard, O. *Chemical Design Automation News* **1993**, *8*, 31–37. For details of this search see ref. 6b and also see ref. 1e.

11. (a) Karlström, G.; Linse, P.; Wallqvist, A.; Jönsson, B. *J. Am. Chem. Soc.* **1983**, *105*, 3777–3782. (b) Burley, S. K.; Petsco, G. A. *J. Am. Chem. Soc.* **1986**, *108*, 7995–8001. (c) Jorgensen, W. L.; Severance, D. L. *J. Am. Chem. Soc.* **1990**, *112*, 4768–4774. (d) Hobza, P.; Selzle, H. L.; Schlag, E. W. *J. Am. Chem. Soc.* **1994**, *116*, 3500–3506.

12. Edge–to–face arene interactions are considered stabilizing (ref. 11), but the origin and magnitude of such interactions have recently come under scrutiny. See (a) Kim, E.; Paliwal, S.; Wilcox, C. S. *J. Am. Chem. Soc.* **1998**, *120*, 11192–11193 and references cited therein. (b) Umezawa, Y.; Tsuboyama, S.; Honda, K.; Uzawa, J.; Nishio, M. *Bull. Chem. Soc. Jpn.* **1998**, *71*, 1207–1213 and references cited therein.

13. O'Donnell, M. J.; Polt, R. L. *J. Org. Chem.* **1982**, *47*, 2663–2666.

14. Purchased from Aldrich Chemical Company.

15. Stork, G.; Leong, A. Y. W.; Touzin, A. M. *J. Org. Chem.* **1976**, *41*, 3491–3493.

16. Eck, G.; Julia, M.; Pfeiffer, B.; Rolando, C. *Tetrahedron Lett.* **1985**, *26*, 4725–4726.

17. Castro, B.; Dormoy, J.–R.; Dourtoglou, B.; Evin, G.; Selve, C.; Ziegler, J.–C. *Synthesis* **1976**, 751–752.